In vivo mechanism of antibody-based immunotherapy

Sow, H.S.

4

CHAPTER 4.

High Fcγ-receptor expression on intratumoral macrophages enhances tumor-targeting antibody therapy

Benonisson H., Sow HS., Breukel C., Claassens J., Brouwers C., Linssen MM., Fransen MF., Sluijter M., Ossendorp F., van Hall T., Verbeek JS.

J. Immunol. 2018 Dec 15; 201 (12): 3741 – 3749. doi:10.4049/jimmunol.1800700 (2018).


TA99 is mIgG2c, okay!!!
Hreinn
This world is crazy
Hreinn
Not good
Hreinn

Abstract

Therapy with tumor-specific antibodies (Abs) is common in the clinic but has limited success against solid malignancies. We aimed at improving the efficacy of this therapy by combining a tumor-specific Ab with immune-activating compounds. In this study, we demonstrate in the aggressive B16F10 mouse melanoma model that concomitant application of the anti-TRP1 Ab (clone TA99) with TLR3-7/8 or -9 ligands, and IL-2 strongly enhanced tumor control in a therapeutic setting. Depletion of NK cells, macrophages, or $CD8^+$ T cells all mitigated the therapeutic response, showing a coordinated immune rejection by innate and adaptive immune cells. FcγRs were essential for the therapeutic effect, with a dominant role for FcγRI and a minor role for FcγRIII and FcγRIV. FcγR expression on NK cells and granulocytes was dispensable, indicating that other tumoricidal functions of NK cells were involved and implicating that FcγRI, -III, and -IV exerted their activity on macrophages. Indeed, $F4/80^+$ $Ly6C^+$ inflammatory macrophages in the tumor microenvironment displayed high levels of these receptors. Whereas administration of the anti-TRP1 Ab alone reduced the frequency of these macrophages, the combination with a TLR agonist retained these cells in the tumor microenvironment. Thus, the addition of innate stimulatory compounds, such as TLR ligands, to tumor-specific Ab therapy could greatly enhance its efficacy in solid cancers via optimal exploitation of FcγRs.

Introduction

Tumor-targeting Ab therapy is an established treatment in cancer, and Abs such as anti-Her2/neu (ErBb2) (trastuzumab, pertuzumab), anti-CD20 (rituximab), and anti-EGFR (cetuximab) are commonly used in the clinic. There are several means by which tumor-targeting Abs can mediate tumor cell killing. The Abs for solid tumors, anti-Her2 (ErBb2) and anti-EGFR, interfere directly with cell signaling by blocking these receptors on the cell surface, resulting in induction of apoptosis. Interaction of the Fc part of Abs with complement can result in the induction of complementdependent cell-mediated phagocytosis and complement-dependent cell-mediated cytotoxicity (1). Another important mechanism is the activation of innate effector cells, such as NK cells, macrophages, and neutrophils, through binding of the Fc region of the Ab to FcγR. FcγR binding initiates downstream effector functions directed toward tumor cells, including Ab-dependent cell-mediated cytotoxicity, Abdependent cell phagocytosis (ADCP), and trogocytosis (2, 3) as well as innate effector functions like release of cytokines and chemokines that can alter the tumor microenvironment (4, 5).

So far, all Food and Drug Administration–approved tumortargeting Abs act via interference with cell signaling (6, 7). To what extent additional activation of innate effector cells contributes to their therapeutic efficacy is difficult to determine in cancer patients. However, several studies have demonstrated a correlation between FcγR polymorphisms influencing the affinity of IgG binding and the therapeutic efficacy of anti-EGFR, anti-HER2/neu, and anti-CD20 Abs (6, 8–10). These data strongly argue for FcγR contribution, in addition to cell signaling interference, to the mode-of-action of these tumor-targeting Abs.

TA99 is a widely used tumor-targeting mouse IgG2a mAb that binds to the protein Trp1 (gp75) expressed at the cell surface of B16F10 tumor cells. Trp1 is not a signaling protein, making it an optimal model to study the role of Ab downstream effector functions. Several publications demonstrated the efficacy of the TA99 Ab in a prophylactic setting, as the treatment started at the same day as injection of the tumor cells (11–15). All these studies demonstrated a crucial role of FcγRs. The clearance of tumor cells, most likely by ADCP, required macrophages that express all activating FcγR (14, 16, 17) or neutrophils expressing FcγRIII and FcγRIV (18). In contrast, application of the TA99 Ab in a therapeutic setting, after a solid tumor is established, had no impact on tumor outgrowth (19). Interestingly, a combination of TA99 with TLR4 agonists or IL-2 with extended half-life had some therapeutic effect, suggesting that there is room for improvement of TA99-based therapy (20–22).

In preclinical studies, TLR agonists are applied in tumor therapy, as they stimulate both adaptive and innate immune responses. It has been shown that they are effective in many mouse models both in combination with other treatments and as monotherapy to induce tumor clearance (23–26). Moreover, a recent phase I clinical trial showed that a TLR8 agonist improved treatment with anti-EGFR Ab (27).

In this study, we investigated the synergy between TA99 with the innate stimulating compounds imiquimod, CpG, poly(I:C), agonistic CD40 Ab, and IL-2 in a therapeutic setting of B16F10 melanoma. We observed a significant increase in survival of mice treated with the combination of TA99, a TLR ligand, and IL-2 compared with untreated mice or mice treated with TA99 alone. The therapeutic effect of this combination depended on $CD8^+$ T cells, NK

cells, and macrophages and activating FcγR. The addition of imiquimod and IL-2 increased the relative proportion of inflammatory macrophages with high expression of FcγR in the tumor microenvironment and, most likely, thereby making the tumor-targeting TA99 Ab more efficacious in elimination of tumor cells.

Materials and Methods

Mice

Mice were housed and all experiments were performed at the specific pathogen–free animal facilities of the laboratory animal facility of the Leiden University Medical Center (LUMC). The health status of the animals was monitored over time. Animals tested negative for all agents listed in the Federation of European Laboratory Animal Science Associations guidelines for specific pathogen–free mouse colonies (28). All mouse studies were approved by the animal ethics committee of the LUMC. Experiments were performed in accordance with the Dutch Act on Animal Experimentation and European Union Directive 2010/63/EU ("on the protection of animals used for scientific purposes"). C57BL/6J mice, both female and male, were purchased from Charles River Laboratories. All FcγR knockout (KO) mice were generated in the transgenic mouse facility of the LUMC: FcγRI 2/2 mice (29), FcγRIII/IV$^{-/-}$ mice (30), and the novel generated FcγRIII/IV$^{fl/fl}$ (Supplemental Fig. 1). FcγRI/III/IV$^{-/-}$ were generated by crossbreeding FcγRI$^{-/-}$ and FcγRIII/IV$^{-/-}$ mice. The EIIaCre deleter strain (n > 20 on C57BL/6J background) was a kind gift of Dr. H. Westphal. The Flp deleter strain C57BL/6-Tg(CAG-lpe)36Ito/ItoRbrc, was purchased from The Jackson Laboratory (Bar Harbor, ME). The hMRP8-Cre strain was provided by Dr. O. Sohnlein as a kind gift of Dr. E. Pasague´, and the Ncr1-Cre strain was a kind gift of Dr. V. Sexl. Both strains were backcrossed into C57BL/6 background. Mice were checked for their genotype by PCR. All mice were used in the age range of 8–12 wk.

Generation of novel conditional FcγRIII/IV$^{fl/fl}$ mouse

For the generation of the conditional FcγRIII/IV double KO mouse (FcγRIII/IV$^{fl/fl}$) on C57BL/6 background, a single LoxP site was introduced in the first intron of the FcγRIII gene by microinjection of a homologous LoxP site containing single-stranded oligodeoxynucleotide, CRISPR single guide RNA, and Cas9 mRNA in the fertilized oocytes of a previously generated FcγRIV$^{fl/fl}$ mouse strain (Supplemental Fig. 1A) (30). The sequence of single guide RNA homologous to intron 1 of FcγRIII gene is 5′-GTTCCAATTCCAGGCCAACC-3′ (underlined position indicates the double strand break). The sequence of single-stranded oligodeoxynucleotide with LoxP site (bold) and NheI restriction site (underlined) is 5′-TGATAGGAGAATCAGGAGTTCAAGGTTAGCTTCAACTATAGTGCGTTCCAATTCC AGGCCGCTAGCA**TAACTTCGTATAGCATACATTATACGAAGTTAT**AACCTGGC TTTGTGAGACCCTGTGAAAAAAAGAGATTTCTAGAGCTGGGTGTGGTGATCG-3′. The obtained offspring were backcrossed two generations into C57BL/6J background and subsequently intercrossed, and mice homozygous for the LoxP site in intron 1 of the FcγRIII gene and the two LoxP sites in the FcγRIV gene were crossed with C57BL/6 hMRP8-Cre or C57BL/6 Ncr1-Cre transgenic mice, resulting in neutrophil-specific and NK cell–specific FcγRIII/IV$^{-/-}$ mice, respectively. The deletion was confirmed by specific PCR (Supplemental

Fig. 1B, 1C). The sequences of the set of primers used were as follows: F3_cr_AB forward: 5′-GGTTTAGAAACCGGGGAGAG-3′, F3_cr_AB reverse: 5′-GACAGCCTTTTCAGGGACTG-3′; F4_geno_null forward: 5′-TAGACTAAAGGTCATGTGTGATC-3′, F4_geno forward: 5′-GGAGGCCAGAAGACTTTTA-3′, F4_geno reverse: 5′-GGAACTGTTTTGGAAGGATT-3′; Mrp8 forward: 5′-CGGTCGATGCAACGAGTGATGAGG-3′, Mrp8 reverse: 5′-CCAGAGACGGAAATCCATCGCTCG-3′; Ncr1 forward: 5′-GACCATGATGCTGGGTTTGGCCCAGATG-3′, Ncr1 reverse: 5′-ATGCGGTGGGCTCTATGGCTTCTG-3′. Neutrophil- and NK cell–specific FcγRIII/IV$^{-/-}$ mice developed normally and showed normal breeding characteristics. There were no evident effects on the homeostasis of the immune system, and the abundance of neutrophils and NK cells in these crossed mice was comparable to that of wild type (WT) mice (Supplemental Fig. 1D). The cell type–specific absence of FcγRIII and FcγRIV on the surface of immune cells was confirmed by flow cytometry using FcγRIII- and FcγRIV-specific Abs (Supplemental Fig. 2).

TA99 tumor therapy

C57BL/6J, FcγRI$^{-/-}$, FcγRIII/IV$^{-/-}$, FcγRI/III/IV$^{-/-}$, Ncr1-Cre × FcγRIII/IV$^{fl/fl}$, hMRP8-Cre × FcγRIII/IV$^{fl/fl}$, and control FcγRIII/IV$^{fl/fl}$ mice were s.c. injected at the left flank with 100,000 B16F10 cells that had been passaged twice after thawing. Mice were treated by i.p. injections of 200 μg of TA99 (mouse IgG2c isolated from TA99 hybridoma) Ab at day 5 and 7 in combination with topical application of 62.5 mg Aldara imiquimod cream (Aldara, 3M Health Care) containing 5% imiquimod at the right flank on shaved skin at day 4 and 11. Mice were anesthetized for few hours with xylazine and ketamine to prevent them from licking the cream. Alternatively, the other TLR ligands, CpG (50 μg oligodeoxynucleotide 1826; InvivoGen) or 50 μg poly(I:C) (Hiltonol; Oncovir) were applied by injecting the mice s.c at the right flank. Mice were injected i.p. with recombinant human IL-2 (6×10^5 IU; Novartis, Breda, the Netherlands) at day 11 and 12 after tumor transplantation.

In the combination of agonistic anti-CD40 Ab (clone FGK) and TA99, C57BL/6J mice were injected i.p. with 200 μg of TA99 at day 5, 10, and 15 and with 80 μg of anti-CD40 i.p at day 8, 13, and 18.

Analysis of tumor-infiltrating immune cells

C57BL/6J mice were injected with 100,000 B16F10 cells. When tumors were around 27 mm^3 in size, mice were treated with imiquimod cream. One day later, mice were injected i.p. with 200 μg of TA99. At day 2, mice were euthanized, and tumors were harvested. The tumor was cut in small pieces and incubated with 0.2 μg Liberase (Roche) for a half hour at 37°C. Single-cell suspensions were made by mincing the tumor through a cell strainer (BD Biosciences). Cells were resuspended in staining buffer (PBS plus 0.5% BSA plus 0.05% sodium azide) and incubated with Abs to Ly-6C (FITC, clone HK1.4), Ly-6G (Alexa Fluor 700, clone 1A8), F4/80 (PE or PE-Cy7, clone Bm8), CD86 (allophycocyanin, clone IT2.2), NK1.1 (PE-Cy7 or PE, clone PK136), CD45 (PE, clone 30-F11), FcγRI (a647, clone X54-5/7.1), FcγRIII (FITC, clone 275003 or AT154-2), FcγRIIb (a647, clone Ly-17.2), CD11b (PB), FcγRIV (FITC, Clone 012), CD4 (FITC, clone RM4-4), CD8 (A700, clone 53-6.7),

CD69 (allophycocyanin, clone H1.2F3) and CD3 (Pacific Blue, clone 17A2) and aminoactinomycin-D. The Abs were acquired from BD Biosciences, BioLegend/Sony, R&D Systems, Sino Biological, or eBioscience. The FcγRIIb-specific Ab was conjugated with an Alexa Fluor 647 labeling kit from Bio-Rad. FcγRIII-FITC of the clone AT154-2 was a kind gift of M.C. Southampton (31).

For intracellular cytokine analysis, splenocytes or tumor cells were washed and stained for cell surface markers as described above. Next, cells were fixed and permeabilized using the intracellular cytokine staining kit (BioLegend) according to the manufacturer's protocol. Next, cells were stained for IFN-γ using the mAb XMG1.2.

Immune cell depletion

C57BL/6J mice were injected i.p. with 100 μg of the mouse IgG2a (PK136) Ab to deplete NK cells and 50 μg of the rat IgG2b anti-CD8 (2.43) and anti-CD4 (GK1.5) to deplete $CD8^+$ and $CD4^+$ T cells, respectively, 2 and 5 d after tumor transplantation and then every 6 d onwards. Mice were injected i.v. and i.p. with 200 μl of control and clodronate liposomes (Liposoma B.V.) at day 3 and then every 5 d onwards. Blood was analyzed to monitor the depletion.

Statistics

Survival between groups was compared using the Kaplan–Meier curves and the log-rank (Mantel–Cox) test. Comparison of individual groups was done by one-way ANOVA or Student t test. All p values <0.05 were considered significant.

Results

Synergistic therapeutic effect of TA99 Ab with imiquimod and IL-2 in B16F10 melanoma

Two subsequent injections of the tumor-targeting mAb TA99 (anti-Trp1/gp75, mouse IgG2a isotype) at day 5 and 7 after transplantation of B16F10 melanoma cells did not induce a therapeutic effect. To improve its therapeutic efficacy, we added immune stimuli to create a therapeutic window. A combination of TRL7/8 agonist imiquimod in the form of Aldara cream application on the shaved skin, IL-2, and TA99 induced a significant increase in survival of B16F10-bearing mice compared with mice treated with TA99 alone or imiquimod/IL-2 or untreated mice (Fig. 1A, 1B). Imiquimod and IL-2 were administered at distant sites and were not targeted directly into the tumor microenvironment, indicating that systemic activation of adaptive and innate immune cells improves the tumor-targeting TA99 Ab therapy. In a subsequent experiment, it was evident that imiquimod provided the strongest support to TA99 because removal of IL-2 but not imiquimod still significantly improved survival (Supplemental Fig. 3). However, addition of IL-2 to this protocol seemed to further boost the combination and was thus included in further studies (Supplemental Fig. 3).

To investigate whether imiquimod cream was unique in this therapy improvement or whether other TLR agonists improved Ab therapy as well, we replaced imiquimod with CpG or poly(I:C), which are agonists of TLR7/8 and TLR3, respectively. Systemic delivery through

s.c injection on a distant site from the tumor injection of these compounds induced a similar effect as imiquimod (Fig. 1C). Similar findings were recently reported with the use of TA99, poly(I:C), and a stabilized form of IL-2 (32). Furthermore, the therapeutic efficacy of TA99 was strongly improved by combination with an agonistic anti-CD40 Ab, a well-known stimulator of innate and adaptive immunity. Addition of anti-CD40 Ab resulted not only in delayed tumor outgrowth but also significantly more long-term survival of animals (Fig. 1D). Thus, activating stimuli of the adaptive and innate immune cells in general can improve tumor-directed Ab therapy.

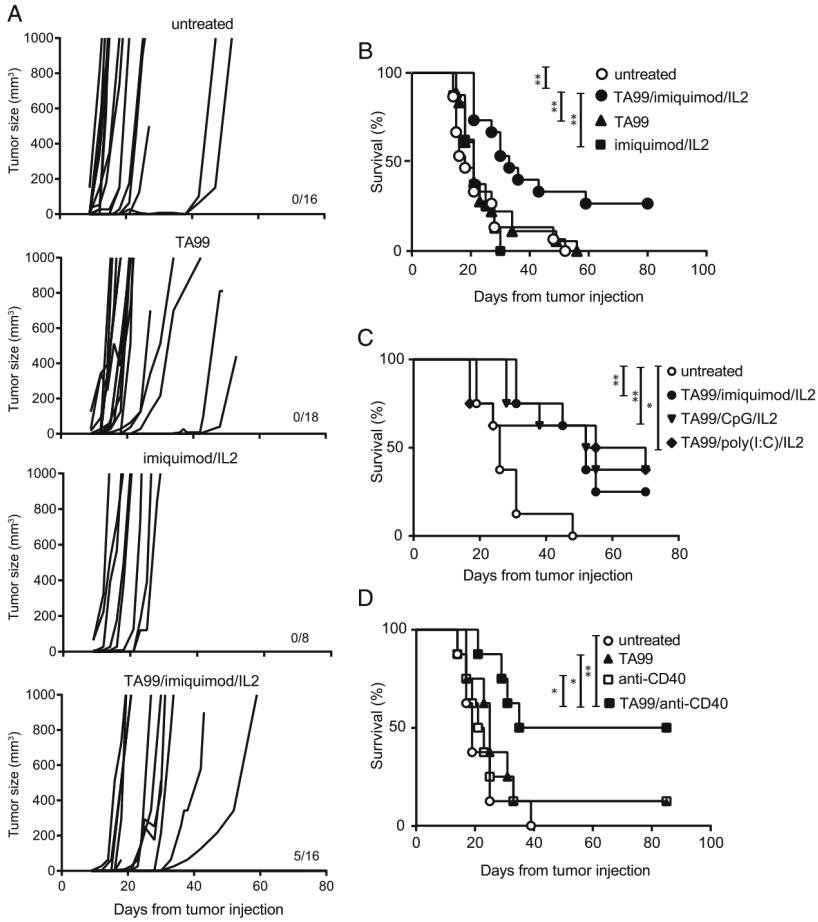

Figure 1. Imiquimod cream and IL-2 enhances the therapeutic efficacy of TA99 in B16F10 mouse model of melanoma. (A) Tumor growth curves of B16F10 melanoma treated with TA99 alone or combinations of imiquimod/IL-2 or TA99/imiquimod/IL-2. Numbers in each graph represent fraction of surviving mice at the end of the experiment at day 80. Compiled data from two independent experiments with similar outcomes are depicted (16–18 mice per group, except for imiquimod/IL-2, n = 8). (B) Kaplan–Meier survival curves of data shown in (A). (C) Kaplan–Meier survival curves of B16F10 melanomas treated with either TA99/imiquimod/IL-2 or in which imiquimod was replaced by CpG or poly(I:C). Experiment performed once, seven to nine mice per group. (D) Kaplan–Meier survival curves of B16F10 melanomas treated with TA99 in combination with agonistic CD40 Ab. Experiment performed three times with similar outcomes, seven to nine mice per group. *p < 0.05, **p 0.01, log-rank analysis.

The therapeutic efficacy of the combination of imiquimod, IL-2, and TA99 Ab depends on CD8$^+$ T cells and FcγRs

To unravel the underlying mechanisms of the synergistic effect of imiquimod, IL-2, and TA99, the combination therapy was tested in mice either depleted for CD8$^+$ or CD4$^+$ T cells or deficient for all three activating FcγRs. Depletion of CD8$^+$ T cells clearly mitigated the effect of the combination therapy, as significantly less survival in CD8$^+$ T cell–depleted mice was observed compared with nondepleted mice. In contrast, CD4$^+$ T cell depletion had no significant effect on survival (Fig. 2A, 2B). The depletion efficiency was monitored on blood cells and reached 100% in all mice (Supplemental Fig. 4A). The combination therapy failed to induce increased survival in B16F10-bearing mice lacking the three activating receptors FcγRI, -III, and -IV (Fig. 2B). In conclusion, in TA99/imiquimod/IL-2 combination therapy, both adaptive immune cells and activating FcγR were essential.

To understand which FcγRs on which immune cells were involved in the mechanism of action, several FcγR KO mouse strains were analyzed. In mice deficient for FcγRI, the therapeutic effect was completely abrogated (Fig. 3A). The treatment effect was also lost in the majority of mice constitutively lacking FcγRIII and FcγRIV, but, still, some mice controlled the melanoma (Fig. 3B). Together, these data suggested that FcγRI was the dominant receptor in this system. It is well documented that FcγRI is expressed exclusively on mononuclear myeloid cells, FcγRIV is expressed on mononuclear myeloid cells and neutrophils, and FcγRIII is expressed on all myeloid cells and NK cells (33). Thus, our observations suggested that FcγRI-expressing mononuclear cells play a dominant role in TA99/imiquimod/IL-2 combination therapy with a minor role for FcγRIII and FcγRIV in yet unidentified innate immune cells.

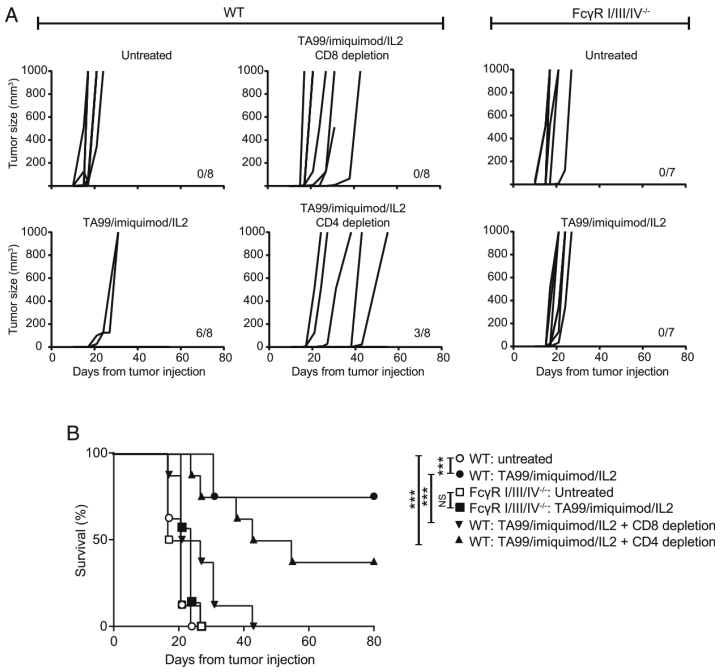

Figure 2. The therapeutic efficacy of TA99/imiquimod/IL-2 combination therapy depends on FcγR and CD8$^+$ T cells. (A) Tumor growth curves of B16F10 melanoma in WT mice (left panels) or in FcγRI/III/IV$^{-/-}$ mice (right panels). WT mice were also depleted for CD4$^+$ or CD8$^+$ T cells before the start of the TA99/imiquimod/IL-2 treatment (middle panels). Numbers in each graph represent fraction of surviving mice at the end of the experiment at day 80. Experiment was performed twice with similar outcomes, seven to eight mice per group. (B) Kaplan–Meier survival curves from data shown in (A). $p < 0.001$, log-rank analysis.

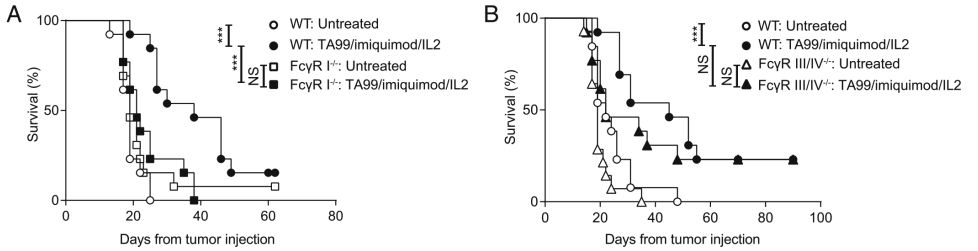

Figure 3. TA99/imiquimod/IL-2 combination therapy is abrogated in FcγRI$^{-/-}$ mice and diminished in FcγRIII/IV$^{-/-}$ mice. (A) Kaplan–Meier survival curves of B16F10 melanoma in WT mice and FcγRI$^{-/-}$ mice. Mice were treated with TA99/imiquimod/IL-2. (B) Kaplan–Meier survival curves of B16F10 melanoma in WT mice and FcγRIII/IV$^{-/-}$ mice. Mice were treated with TA99/imiquimod/IL-2. For both experiments, 12–14 mice per group from two comparable experiments were included. ***$p < 0.001$, log-rank analysis.

FcγRIII-independent role of NK cells in the combined therapy

NK cells only express FcγRIII and are capable of killing tumor cells via Ab-dependent cell-mediated cytotoxicity (34). Because FcγRIII and -IV were involved in the combination therapy and imiquimod is known to activate NK cells (23), we tested the influx and activation of NK cells in the tumor microenvironment by flow cytometry. NK cells were present in B16F10 tumors, and 3 d after imiquimod application, the proportion of NK cells seemed to be higher (Fig. 4A, 4B). Importantly, a significantly higher proportion of CD69-expressing activated NK cells were observed in B16F10 tumors (Fig. 4A, 4B), confirming previous data (23). To better understand the contribution of NK cells to the combination therapy, NK cells were depleted with anti-NK1.1 Abs during the therapy (Fig. 4C). Efficient depletion was confirmed on blood samples (Supplemental Fig. 4B). The survival was significantly lower compared with survival of nondepleted mice, but the therapeutic effect was not completely gone (Fig. 4C), demonstrating a minor contribution of NK cells. To determine whether this role of NK cells was FcγRIII dependent, we made use of mice deficient for FcγRIII exclusively on NK cells: Ncr1-Cre × FcγRIII/IV$^{fl/fl}$ mice (Supplemental Figs. 1, 2). NK-specific FcγRIII deficiency had no effect on the therapeutic efficacy of the combination therapy (Fig. 4D), and we concluded that other effector mechanisms of NK cells were involved. Alternate effector mechanisms of NK cells include release of cytokines, and imiquimod application, indeed, systemically induced IFN-γ release by NK cells and also led to higher frequencies of IFN-γ producing NK cells in the local tumor environment (Fig. 4E). In summary, our data indicate that NK cells contribute to the therapeutic effect of the combination therapy independent of FcγRIII.

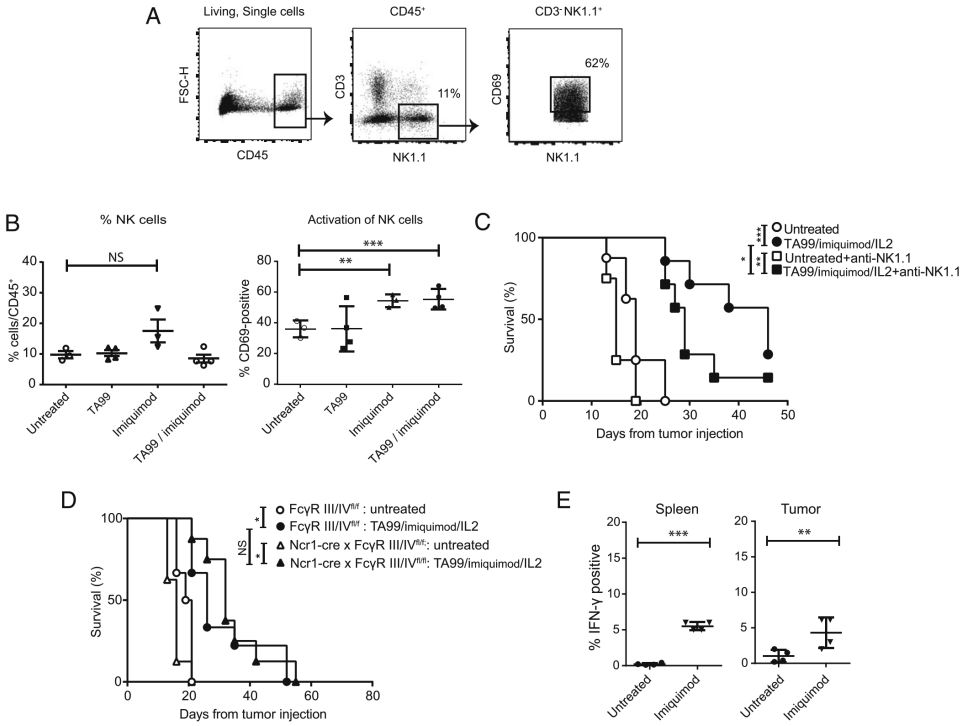

Figure 4. NK cells contribute to the efficacy of TA99/imiquimod/IL-2 therapy independent of FcγRIII. (A) B16F10 tumors were harvested from mice and enzymatically dispersed before analysis by flow cytometry. Gating strategy is shown for NK cells. (B) Tumor infiltration frequency and activation status (CD69 expression) of NK cells were determined by flow cytometry. Each symbol represents one mouse, seven to nine mice per group. Experiment performed twice with comparable outcomes. Means and SEM shown. $^{**}p < 0.01$, $^{***}p < 0.001$, one-way ANOVA. (C) Kaplan–Meier survival curve of treated B16F10 melanoma in WT mice depleted for NK cells (anti-NK1.1). Experiment performed twice with similar outcomes, seven to nine mice per group. $^{*}p < 0.05$, $^{**}p < 0.01$, $^{***}p < 0.001$, log-rank analysis. (D) Kaplan–Meier survival curve of B16F10 melanoma in mice lacking FcγRIII in NK cells (Ncr1-Cre x FcγRIII/IV$^{fl/fl}$ mice) and FcγRIII/IVfl/fl control mice. Experiment performed once, seven to nine mice per group. Log-rank analysis. $^{*}p < 0.05$. (E) Expression of IFN-γ by NK cells from spleen and tumor in WT mice determined by flow cytometry. Means and SEM shown. $^{**}p < 0.01$, $^{***}p < 0.001$, Student t test.

Improvement of anti-Trp1 therapy by imiquimod is mediated by mononuclear cells but not neutrophils

In addition to NK cells, other innate immune cells expressing activating FcγR were present in the microenvironment of B16F10 tumors. To get insight in the dynamics of these cells in response to the treatment, the immune infiltrates of tumors were analyzed by flow cytometry 3 d after the start of treatment. Comparisons of single treatment allowed us to determine the intrinsic effect of imiquimod. No gross changes were observed in the frequencies of total immune cells (CD45$^+$ cells) or total myeloid cells (CD11b$^+$ cells) (Fig. 5A). We then examined myeloid cell subsets and discerned inflammatory macrophages (CD45$^+$CD11b$^+$F4/80$^+$Ly-6C$^+$), stationary macrophages (CD45$^+$CD11b$^+$F4/80$^+$Ly-6C$^-$), and neutrophils (CD45$^+$CD11b$^+$F4/80$^-$Ly-6G$^+$). Frequencies of neutrophils seemed to decrease after Ab or

imiquimod administration, but these differences were not statistically significant (Fig. 5B). Importantly, imiquimod did enhance the proportion of inflammatory macrophages at the expense of stationary macrophages (Fig. 5B). The proportion of these inflammatory macrophages decreased after therapy with TA99 alone (Fig. 5B), most likely also decreasing downstream effector functions of TA99. Importantly, application of imiquimod corrected these decreased frequencies and resulted in sustained high proportion of these myeloid immune cells (Fig. 5B).

We then analyzed the FcγR expression levels by these three different myeloid cell subsets in the tumor and found that inflammatory macrophages displayed much higher levels of all four FcγRs than stationary macrophages and neutrophils (Fig. 5C). Neutrophils only expressed FcγRIII and FcγRIV, and we determined the role of these two activating receptors on neutrophils by using hMRP8-Cre × FcγRIII/IV$^{fl/fl}$ mice, which selectively lack FcγRIII and FcγRIV on this myeloid subset (Supplemental Fig. 2). Neutrophil-specific FcγR deficiency had no effect on survival (Fig. 5D), indicating that neutrophils did not play a FcγR-dependent role in the combination therapy. Together, these results implied an important contribution of mononuclear cells, most likely inflammatory macrophages, and their activating FcγR to this Ab combination therapy.

Knowing that imiquimod retained high proportions of inflammatory macrophages in the tumor environment (Fig. 5B) and that these myeloid cells displayed the highest FcγR levels of all myeloid subsets (Fig. 5C), we were interested in gaining insight into the differentiation direction of these cells. Application of imiquimod strongly enhanced the expression of CD86 on inflammatory macrophages, whereas the expression levels of this T cell costimulatory ligand did not alter on other myeloid subsets (Fig. 6A). These data suggested that imiquimod either polarized tumor-resident macrophages toward M1-like phenotypes or promoted an influx of M1-like macrophages. Of note, imiquimod boosted the presence of activating FcγRs, including the involved high-affinity FcγRI (Fig. 2A), in the tumor environment. To confirm the essential role of macrophages during combination therapy, we depleted them using clodronate liposomes (Fig. 6B, 6C). Tumor outgrowth was clearly hastened in TA99- and imiquimod-treated mice after macrophage depletion and percentages of long-term surviving mice were lower compared with mice with control liposomes. Efficiency of macrophage depletion was validated during the experiment (Supplemental Fig. 4C).

In summary, our data indicate that systemic application of immune stimuli improve tumor-targeting Abs in a therapeutic setting of established melanoma. This combination therapy depends on adaptive immune cells (CD8$^+$ T cells), innate lymphocytes (NK cells), and activating FcγR on intratumoral inflammatory macrophages.

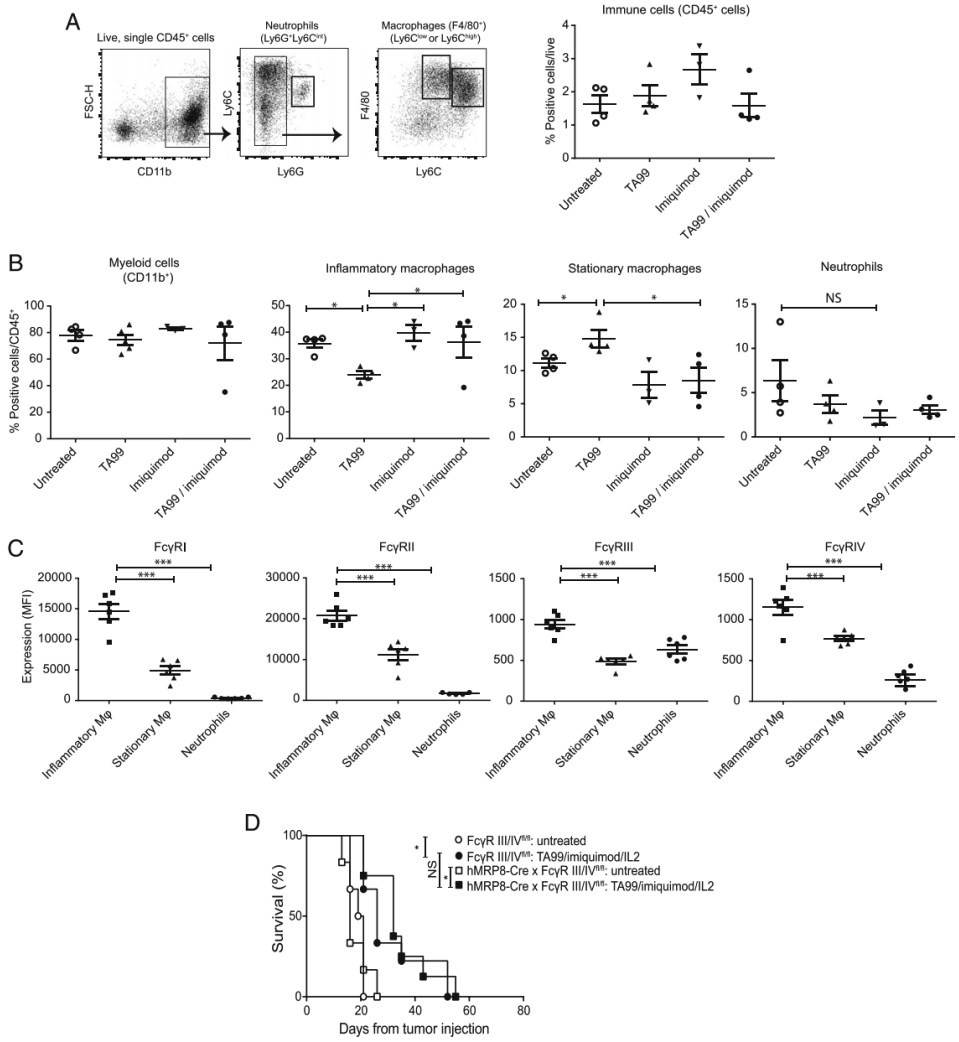

Figure 5. Imiquimod sustains the infiltration of highly FcγR-positive inflammatory macrophages. (A) B16F10 tumors were harvested from mice and enzymatically dispersed before analysis by flow cytometry. Gating strategy is shown for myeloid cells, and frequencies of all $CD45^+$ cells out of live cells are shown. (B) B16F10 melanomas were treated with imiquimod (3d before) or with TA99 (2d before) or a combination of both. Frequencies of intratumoral total myeloid cells ($CD11b^+$ out of all $CD45^+$ cells) and the myeloid subsets "inflammatory macrophages" ($CD45^+$ $CD11b^+$ $F4/80^+$ $Ly\text{-}6C^{high}$), stationary macrophages ($CD45^+$ $CD11b^+$ $F4/80^+Ly\text{-}6C^{low}$), and neutrophils ($CD45^+$ $CD11b^+$ $Ly\text{-}6G^+$ $Ly\text{-}6C^{int}$) were determined. Means and SEM from one representative experiment out of two is shown. *$p < 0.05$, one-way ANOVA. (C) Expression levels of FcgRI, FcgRII, FcgRIII, and FcgRIV on tumorinfiltrating myeloid subsets. Means and SEM are shown from one out of two similar experiments. ***p , 0.001, one-way ANOVA. (D) Kaplan–Meier survival curve of B16F10 melanoma in mice that selectively lack FcgRIII and IV on neutrophils (hMRP8Cre 3 FcgRIII/IV2/2 mice) and FcgRIII/IVfl/fl control mice. Experiment performed twice with similar outcomes, shown are six to eight animals per group. *$p < 0.05$, log-rank analysis.

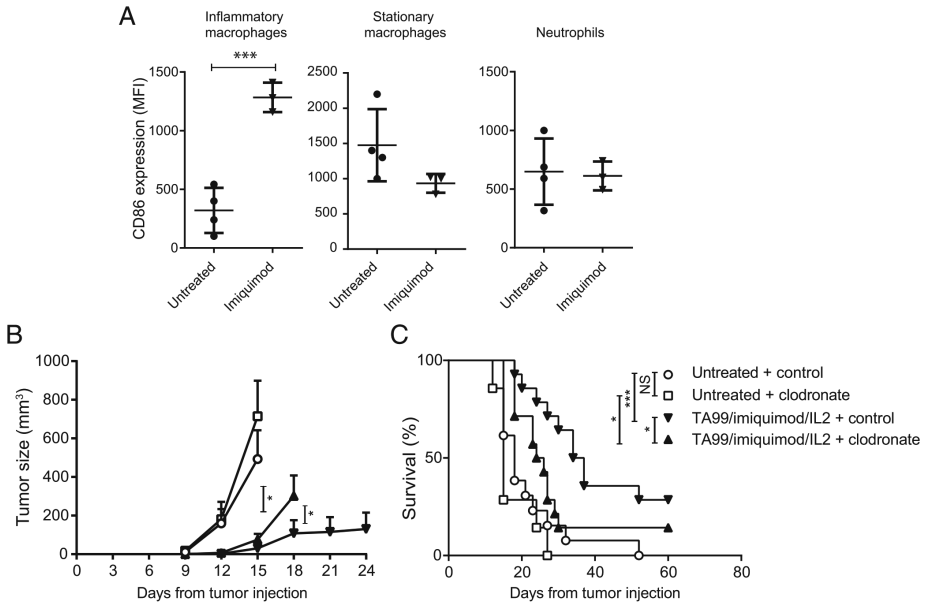

Figure 6. Macrophages are indispensable for TA99/imiquimod/IL-2 therapy in B16F10 melanoma model. (A) Expression of CD86 by tumor-infiltrating inflammatory macrophages, stationary macrophages, and neutrophils in WT mice measured by flow cytometry. Means and SEM shown from four animals per group. ***$p < 0.001$, Student t test. (B) Average tumor growth curves and (C) Kaplan–Meier curves of B16F10-bearing WT mice treated with TA99/imiquimod/IL-2 in the presence of clodronate or control liposomes. Average growth curves in (B) were terminated at the moment the first mouse tumor reached its maximum size of 1000 mm^3. Results are shown from two pooled experiments, 14–16 mice per group. One-way ANOVA (B) and log-rank analysis (C). *$p < 0.05$, ***$p < 0.001$.

Discussion

In this study, we report on combination therapy based on tumor-targeting Abs. Addition of several TLR agonists or agonistic CD40 improved the therapy of established B16F10 melanoma. The increased therapeutic efficacy depended on CD8 T cells and FcγR expression on macrophages, with a minor FcγR-independent role of NK cells. Addition of imiquimod cream resulted in a relative increase of inflammatory macrophages that highly express FcγRs in the tumor microenvironment.

In all studies investigating the role of FcγR in TA99 therapy in the B16F10 model, the Ab was injected on the same day as the tumor was transplanted. Different laboratories reported contradictory results from their analysis of the role of activating FcγR using different panels of $Fc\gamma R^{-/-}$ mice and FcγR-blocking Abs. Some of these differences between the studies can probably be attributed to variations in experimental conditions, like location of the tumor and production process of the TA99 Ab. When B16F10 was seeded in lung (13, 15) and liver (14), a prominent role for FcγRI was found (13) together with FcγRIV (14) or FcγRIII (15). Lehmann et al. (17) showed that the location of the tumor determines what macrophage subset mediates ADCP of tumor cells. The s.c. transplanted B16F10 model required Ly-$6C^{high}$ inflammatory

macrophages, whereas CCL2-independent but CSF2-dependent stationary lung macrophages were required for the treatment of tumors in the lung. Importantly, our study was performed in a therapeutic setting with established s.c. growing B16F10 tumors and provides new insight in the FcγR dependencies. In this study, we show that treatment with TA99 alone of an s.c. transplanted solid B16F10 tumor decreases the relative amount of Ly-6C$^+$ macrophages within the tumor microenvironment, whereas in the combination therapy of TA99 and imiquimod cream, this cellular subset remained constant. Lehmann et al. (17) showed that the influx of Ly-6C$^+$ monocytes depends on CCL2, and others demonstrated that imiquimod induces CCL2-mediated migration of plasmacytoid dendritic cells into the tumor microenvironment (35), which could as well fit our results, as clodronate predominantly depletes macrophages in the spleen and liver, which would thus prevent recruitment to the tumor. This suggests that imiquimod can induce migration of CCL2-attracted myeloid cells into the tumor microenvironment, which is in concordance with a previous study that showed a requirement of CCL2-signaling for TA99-dependent killing of tumor cells in an s.c. tumor setting. These authors showed that the CCL2-mediated effect was dependent on FcγRI and FcγRIV (17), which is in agreement with our study.

In a variety of tumor-targeting Ab monotherapy models, it has been shown that CD8$^+$ T cells are required (36–40). CD8 T cells were, however, not involved in most TA99 monotherapy of B16F10 melanoma in a prophylactic model (41). More effective combination therapies based on TA99, in which immune stimulating factors such as stabilized IL-2 (Fc–IL-2), TLR4 agonist, peptide vaccination, or anti–PD-L1 were supplemented, controlled tumor outgrowth in the therapeutic setting and depended on CD8$^+$ T cells (20, 22). The induction of adaptive immunity depended on cross-presentation by host APCs of Ab/Ag complexes, as treatment was abrogated in mice with impaired cross-presentation capacity (22). As our study also showed the same need for CD8$^+$ T cells, cross-presentation is most likely an underlying mechanism in our therapeutic protocol. In a previous study, in which the combination of imiquimod cream with IL-2 was examined in the RMA/S tumor model, we showed induction of tumor-specific CD4$^+$ and CD8$^+$ T cell responses. Because the RMA/S tumor contains a defect in presenting tumor Ags to CD8$^+$ T cells, only NK cells and CD4$^+$ T cells contributed to the therapeutic efficacy in that model (23). In our current study, CD8$^+$ T cell responses were effective because of the presentation of tumor Ags by MHC class I molecules on the B16F10 melanoma cells. A partial role for CD4 T cells and NK cells was observed in the B16F10 model (Figs. 2A, 2B, 4C, respectively). The contribution of NK cells did not seem to be related to their FcγRIII, as cell lineage-specific KO mice responded equally well to therapy. CD16-mediated immune effector functions seem to be, nonetheless, much weaker in mice compared with humans (42). IFN-γ production by NK cells was apparent in the tumor environment (Fig. 4E), and this cytokine is pivotal for cytostatic effects in tumors, enhancing Ag presentation and upregulation of immune receptors, such as FcγR and CD86 on macrophages (43, 44). In both these studies, imiquimod and IL-2 were systemically administered at the opposing flank of the B16F10 melanoma. Future investigations need to reveal whether the therapeutic effect is stronger when the TLR ligand is applied topically, as clinical application of an imiquimod cream administered topically on a melanoma showed increased migration of T cells into the tumor (45). Importantly, the combination of imiquimod with IL-2 seems to strongly promote T cell activation and induction of tumor-specific immunity.

In conclusion, we have shown that a combination therapy of TA99 and TLR agonist significantly increased survival of B16F10 tumor–bearing mice and that this depended on FcγRs, macrophage recruitment, and $CD8^+$ T cells. This demonstrated that, even with a highly aggressive solid tumor, strong therapeutic effects can be achieved by a tumor- targeting Ab when combined with immune stimulating compounds.

Supplementary Figures

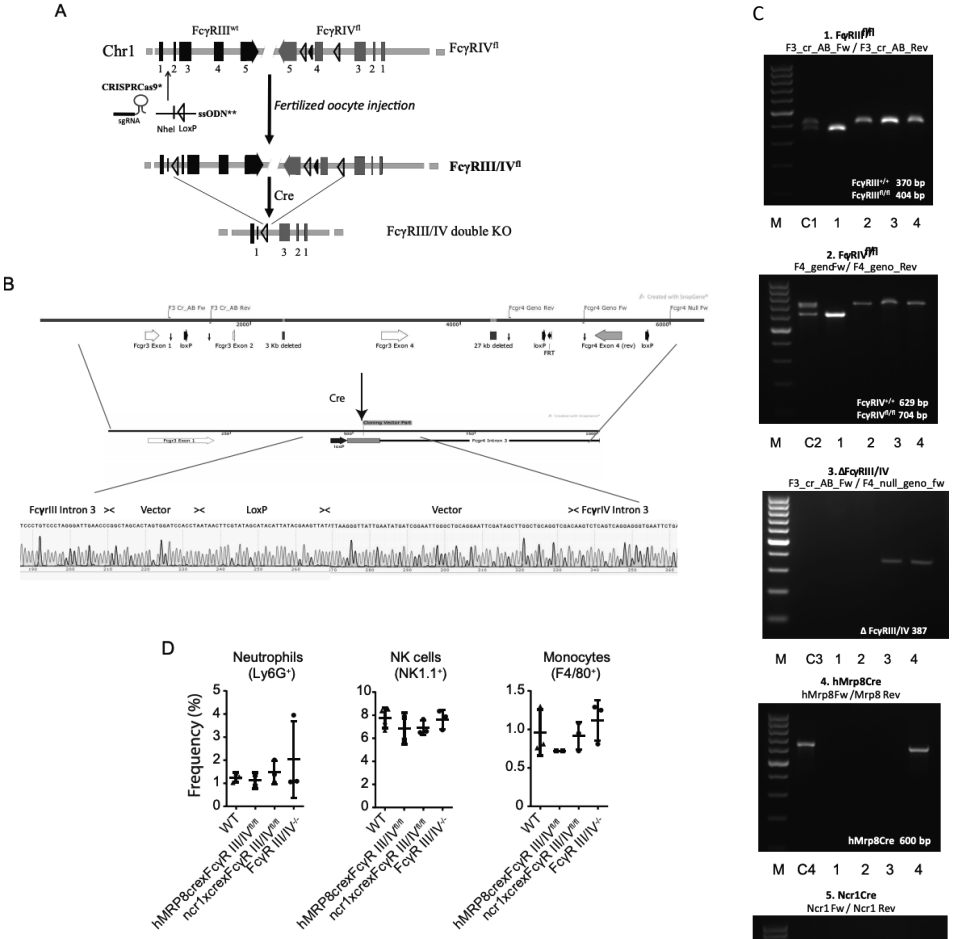

Supplementary Figure S1. Generation and genotyping of a floxed FcγRIII/IV allele using CRISPRCas9. (A) The genomic structure of FcγRIII/FcγRIV gene cluster and indicated CRISPR sgRNA targeting intron one and the ssODN containing the loxP site and additional NheI restriction site. The FcγRIII/IVfl allele and the genomic structure after Cre mediated recombination resulting in the deletion of a 33.7 kb DNA fragment between the most distal LoxP sites. Closed rectangles: exons. EC1 and EC2: extra cellular domain1 and 2 encoding exons; TM/C: transmembrane and cytoplasmic domain encoding exon. Open triangles: LoxP sites; closed triangles: FRT sites. sgRNA and ssODN sequences are given in Material and Methods. (B) Schematic presentation of the FcγRIII/IV locus. Exons are presented as open arrows, LoxP sites as large closed arrows and one Frt site as small closed arrow. Plasmid vector sequences remaining from the cloning procedure presented as gray rectangle. At the bottom: Core sequence of a unique 387 bp PCR fragment flanking the remaining LoxP site and spanning a 33.7 kb deletion in FcγRIII/IV KO cells. (C) Genotyping by PCR as shown on agarose gels. Headings indicate the used primer pairs and the identified gene. At the bottom right of each panel are shown the size of the PCR fragments. Genomic DNA was isolated from the spleens of 1: C57BL/6; 2: FcγRIII/IV$^{fl/fl}$; 3: Ncr1CrexFcγRIII/IV$^{fl/fl}$; 4: hMrp8CrexFcγRIII/IV$^{fl/fl}$. Control DNA was isolated from C1: FcγRIII$^{fl/+}$; C2: FcγRIV$^{fl/+}$; C4: hMrp8Cre^{+} ; C5: Ncr1Cre^{+} . C3: H_20 control. M: 100bp ladder. (D) Shows frequencies of neutrophils (CD11b^{+} F4/80^{-} Ly6G^{+}), NK cells (CD3^{-} NK1.1^{+}) and monocytes (CD11b^{+} F4/80^{+}) in spleens of the indicated mouse strains.

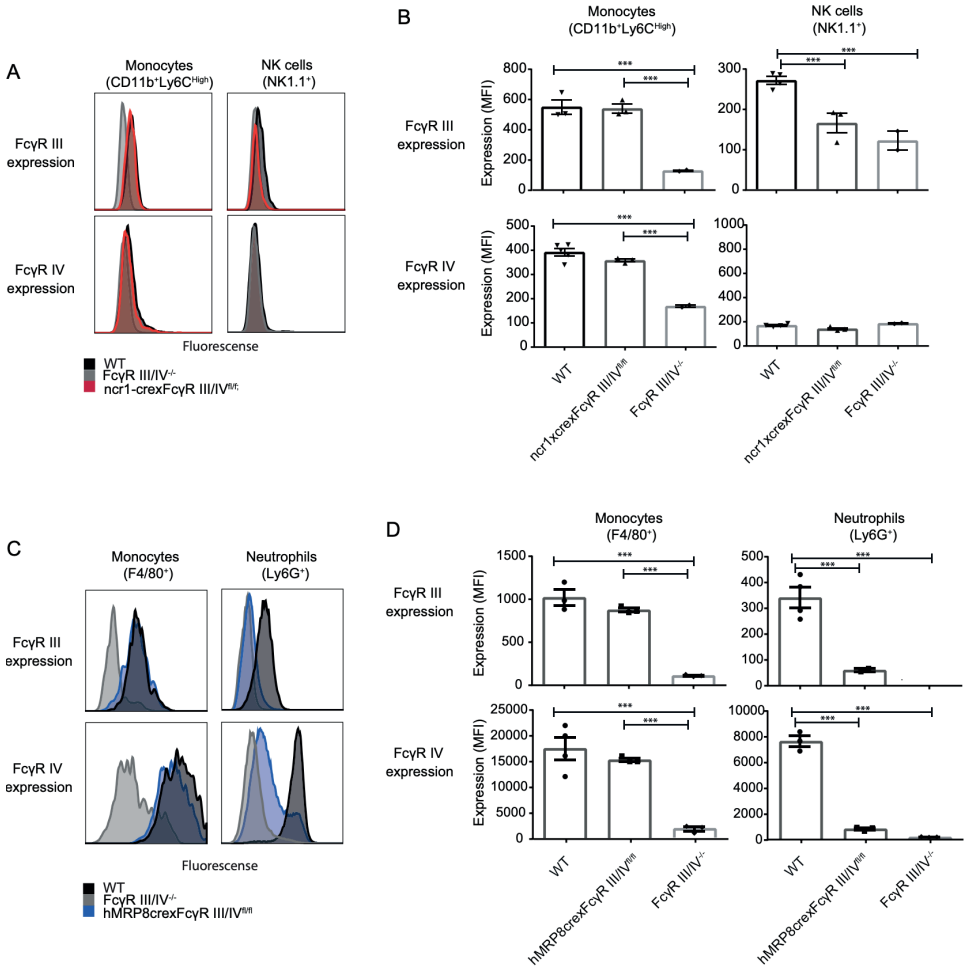

Supplementary Figure S2. Expression analysis of FcγRs in the conditional knockout mice. A-B. Expression of FcγRIII (stained with monoclonal antibody clone AT154-2) and FcγRIV measured by flow cytometry on monocytes and NK cells in blood of WT C57BL/6, Ncr1-cre x FcγRIII/IV$^{fl/fl}$ and FcγRIII/IV$^{-/-}$ mice. Overlapping histograms (A) and average mean fluorescence (MFI) depicted in bar graphs for four animals (B). Geometric mean fluorescence and SEM are depicted. One way Anova, (***p<0.001).C-D. Expression of FcγRIII (stained with monoclonal antibody clone AT154-2) and FcγRIV measured by flow cytometry on monocytes and neutrophils in bone marrow of WT C57BL/6, hMrp8-cre x FcγRIII/IV$^{fl/fl}$ and FcγRIII/IV$^{-/-}$ mice. Overlapping histograms (C) and average mean fluorescence (MFI) depicted in bar graphs for four animals (D). Overlapping histograms (C) and average mean fluorescence (MFI) depicted in bar graphs for four animals (D). Geometric mean fluorescence and SEM are depicted. One way Anova, (***p<0.001). All experiments were repeated twice with similar outcome.

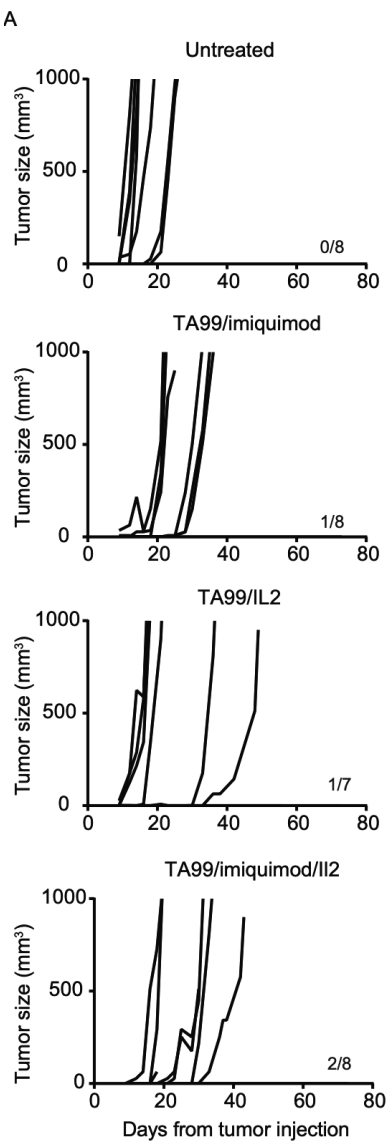

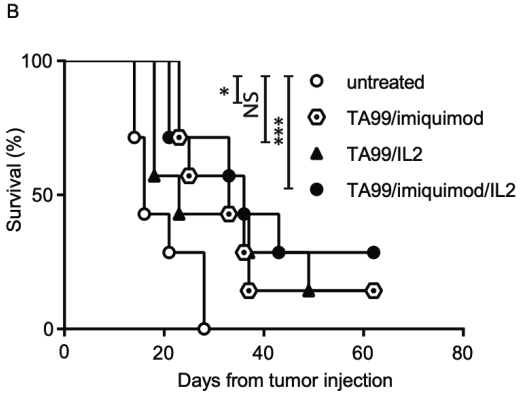

Supplementary Figure S3. Separate contributions of imiquimod and IL-2 to the combination treatment. (A) Tumor growth curves of B16F10 melanoma in WT mice treated with TA99/imiquimod, TA99/IL-2 or the combination of these three components. Numbers at the bottom right represent fraction of surviving mice at the end of the experiment at day 80. (B) Kaplan-Meier survival curves of experiment shown in A, Log-rank analysis. (NS: not significant; *p<0.001).

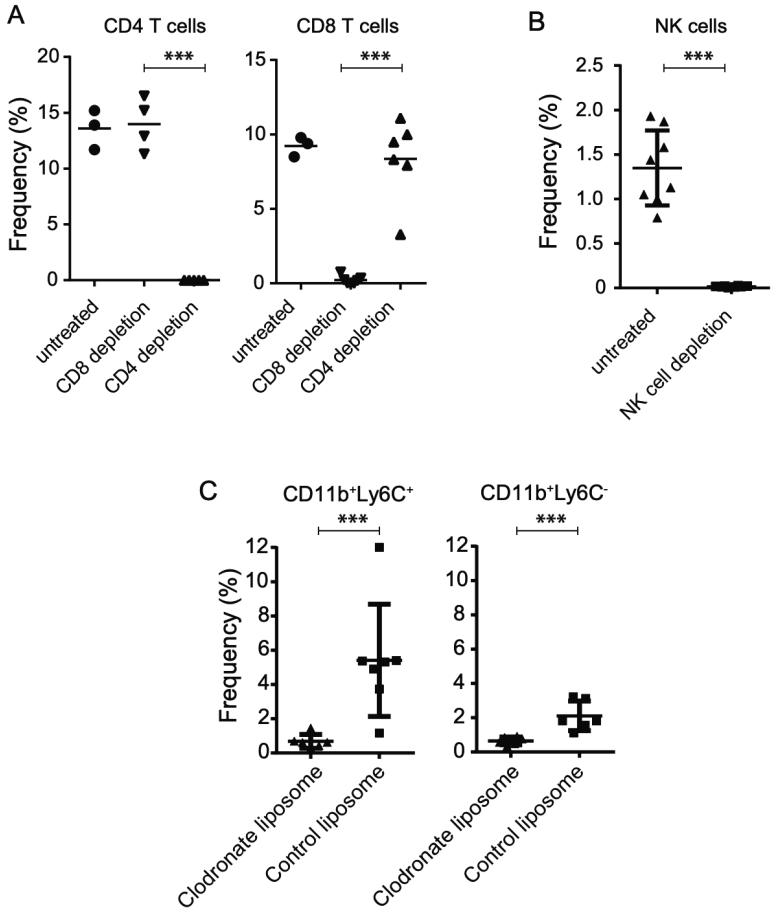

Supplementary Figure S4. Confirmation of *in vivo* depletion studies. (A) Frequencies of $CD4^+$ and $CD8^+$ T cells in blood (out of $CD45^+$ cells) after injection of depleting antibodies to CD4 or CD8 (2 and 7 days before). Shown are 3-8 animals per group, one way Anova (***$p<0.001$). (B) Frequencies of NK cells in blood (out of $CD45^+$ cells) after injection of depleting antibodies to NK1.1 (2 and 7 days before). Shown are 8 animals per group, one way student t-test (***$p<0.001$). (C) Frequencies of monocytes in the blood (out of $CD45^+$ cells) after administration of clodronate liposomes or control liposomes. Two populations of monocytes were analysed: $CD11b^+$ $Ly6C^+$ and $CD11b^+$ $Ly6C^-$.

References

1. Lee, C. H., G. Romain, W. Yan, M. Watanabe, W. Charab, B. Todorova, J. Lee, K. Triplett, M. Donkor, O. I. Lungu, et al. 2017. IgG Fc domains that bind C1q but not effector Fcg receptors delineate the importance of complement-mediated effector functions. Nat. Immunol. 18: 889–898.
2. Valgardsdottir, R., I. Cattaneo, C. Klein, M. Introna, M. Figliuzzi, and J. Golay. 2017. Human neutrophils mediate trogocytosis rather than phagocytosis of CLL B cells opsonized with anti-CD20 antibodies. Blood 129: 2636–2644.
3. Velmurugan, R., D. K. Challa, S. Ram, R. J. Ober, and E. S. Ward. 2016. Macrophage-mediated trogocytosis leads to death of antibody-opsonized tumor cells. Mol. Cancer Ther. 15: 1879–1889.
4. Vogelpoel, L. T., I. S. Hansen, T. Rispens, F. J. Muller, T. M. van Capel, M. C. Turina, J. B. Vos, D. L. Baeten, M. L. Kapsenberg, E. C. de Jong, and J. den Dunnen. 2014. Fc gamma receptor-TLR cross-talk elicits pro-inflammatory cytokine production by human M2 macrophages. Nat. Commun. 5: 5444.
5. Vogelpoel, L. T., I. S. Hansen, M. W. Visser, S. Q. Nagelkerke, T. W. Kuijpers, M. L. Kapsenberg, E. C. de Jong, and J. den Dunnen. 2015. FcgRIIa cross-talk with TLRs, IL-1R, and IFNgR selectively modulates cytokine production in human myeloid cells. Immunobiology 220: 193–199.
6. Scott, A. M., J. D. Wolchok, and L. J. Old. 2012. Antibody therapy of cancer. Nat. Rev. Cancer 12: 278–287.
7. Sliwkowski, M. X., and I. Mellman. 2013. Antibody therapeutics in cancer. Science 341: 1192–1198.
8. Weng, W. K., and R. Levy. 2003. Two immunoglobulin G fragment C receptor polymorphisms independently predict response to rituximab in patients with follicular lymphoma. J. Clin. Oncol. 21: 3940–3947.
9. Musolino, A., N. Naldi, B. Bortesi, D. Pezzuolo, M. Capelletti, G. Missale, D. Laccabue, A. Zerbini, R. Camisa, G. Bisagni, et al. 2008. Immunoglobulin G fragment C receptor polymorphisms and clinical efficacy of trastuzumab-based therapy in patients with HER-2/neu-positive metastatic breast cancer. J. Clin. Oncol. 26: 1789–1796.
10. Pander, J., M. Heusinkveld, T. van der Straaten, E. S. Jordanova, R. Baak-Pablo, H. Gelderblom, H. Morreau, S. H. van der Burg, H. J. Guchelaar, and T. van Hall. 2011. Activation of tumor-promoting type 2 macrophages by EGFRtargeting antibody cetuximab. Clin. Cancer Res. 17: 5668–5673.
11. Nimmerjahn, F., and J. V. Ravetch. 2005. Divergent immunoglobulin g subclass activity through selective Fc receptor binding. Science 310: 1510–1512.
12. Nimmerjahn, F., A. Lux, H. Albert, M. Woigk, C. Lehmann, D. Dudziak, P. Smith, and J. V. Ravetch. 2010. FcgRIV deletion reveals its central role for IgG2a and IgG2b activity in vivo. Proc. Natl. Acad. Sci. USA 107: 19396–19401.
13. Bevaart, L., M. J. Jansen, M. J. van Vugt, J. S. Verbeek, J. G. van de Winkel, and J. H. Leusen. 2006. The high-affinity IgG receptor, FcgammaRI, plays a central role in antibody therapy of experimental melanoma. Cancer Res. 66: 1261–1264
14. Otten, M. A., G. J. van der Bij, S. J. Verbeek, F. Nimmerjahn, J. V. Ravetch, R. H. Beelen, J. G. van de Winkel, and M. van Egmond. 2008. Experimental antibody therapy of liver metastases reveals functional redundancy between Fc gammaRI and Fc gammaRIV. J. Immunol. 181: 6829–6836.
15. Albanesi, M., D. A. Mancardi, L. E. Macdonald, B. Iannascoli, L. Zitvogel, A. J. Murphy, M. Dae¨ron, J. H. Leusen, and P. Bruhns. 2012. Cutting edge: FcgRIII (CD16) and FcgRI (CD64) are responsible for anti-glycoprotein 75 monoclonal antibody TA99 therapy for experimental metastatic B16 melanoma. [Published erratum appears in 2013 J. Immunol. 190: 1381.] J. Immunol. 189: 5513–5517.
16. Gu¨l, N., L. Babes, K. Siegmund, R. Korthouwer, M. Bo¨gels, R. Braster, G. Vidarsson, T. L. ten Hagen, P. Kubes, and M. van Egmond. 2014. Macrophages eliminate circulating tumor cells after monoclonal antibody therapy. J. Clin. Invest. 124: 812–823.
17. Lehmann, B., M. Biburger, C. Bru¨ckner, A. Ipsen-Escobedo, S. Gordan, C. Lehmann, D. Voehringer, T. Winkler, N. Schaft, D. Dudziak, et al. 2017. Tumor location determines tissue-specific recruitment of tumor-associated macrophages and antibody-dependent immunotherapy response. Sci. Immunol. 2: eaah6413.
18. Albanesi, M., D. A. Mancardi, F. Jo¨nsson, B. Iannascoli, L. Fiette, J. P. Di Santo, C. A. Lowell, and P. Bruhns. 2013. Neutrophils mediate antibody-induced antitumor effects in mice. Blood 122: 3160–3164.
19. Ly, L. V., M. Sluijter, S. H. van der Burg, M. J. Jager, and T. van Hall. 2013. Effective cooperation of monoclonal antibody and peptide vaccine for the treatment of mouse melanoma. J. Immunol. 190: 489–496.
20. Zhu, E. F., S. A. Gai, C. F. Opel, B. H. Kwan, R. Surana, M. C. Mihm, M. J. Kauke, K. D. Moynihan, A. Angelini, R. T. Williams, et al. 2015. Synergistic innate and adaptive immune response to combination immunotherapy with anti-tumor antigen antibodies and extended serum half-life IL-2. Cancer Cell 27: 489–501.
21. Wang, S., I. A. Astsaturov, C. A. Bingham, K. M. McCarthy, M. von Mehren, W. Xu, R. K. Alpaugh, Y. Tang, B. A. Littlefield, L. D. Hawkins, et al. 2012. Effective antibody therapy induces host-protective antitumor immunity that is augmented by TLR4 agonist treatment. Cancer Immunol. Immunother. 61: 49–61.
22. Moynihan, K. D., C. F. Opel, G. L. Szeto, A. Tzeng, E. F. Zhu, J. M. Engreitz, R. T. Williams, K. Rakhra, M. H. Zhang, A. M. Rothschilds, et al. 2016. Eradication of large established tumors in mice by combination immunotherapy that engages innate and adaptive immune responses. Nat. Med. 22: 1402–1410.
23. Doorduijn, E. M., M. Sluijter, D. C. Salvatori, S. Silvestri, S. Maas, R. Arens, F. Ossendorp, S. H. van der Burg, and T. van Hall. 2017. CD4+ T cell and NK cell interplay key to regression of MHC class Ilow tumors upon TLR7/8 agonist therapy. Cancer Immunol. Res. 5: 642–653.

24. Stone, G. W., S. Barzee, V. Snarsky, C. Santucci, B. Tran, R. Langer, G. T. Zugates, D. G. Anderson, and R. S. Kornbluth. 2009. Nanoparticledelivered multimeric soluble CD40L DNA combined with Toll-like receptor agonists as a treatment for melanoma. PLoS One 4: e7334.
25. Broomfield, S. A., R. G. van der Most, A. C. Prosser, S. Mahendran, M. G. Tovey, M. J. Smyth, B. W. Robinson, and A. J. Currie. 2009. Locally administered TLR7 agonists drive systemic antitumor immune responses that are enhanced by anti-CD40 immunotherapy. J. Immunol. 182: 5217–5224.
26. Davis, M. B., D. Vasquez-Dunddel, J. Fu, E. Albesiano, D. Pardoll, and Y. J. Kim. 2011. Intratumoral administration of TLR4 agonist absorbed into a cellular vector improves antitumor responses. Clin. Cancer Res. 17: 3984–3992.
27. Chow, L. Q. M., C. Morishima, K. D. Eaton, C. S. Baik, B. H. Goulart, L. N. Anderson, K. L. Manjarrez, G. N. Dietsch, J. K. Bryan, R. M. Hershberg, et al. 2017. Phase Ib trial of the Toll-like receptor 8 agonist, motolimod (VTX2337), combined with cetuximab in patients with recurrent or metastatic SCCHN. Clin. Cancer Res. 23: 2442–2450.
28. Felasa working group on revision of guidelines for health monitoring of rodents rabbits, M. Mahler Convenor, M. Berard, R. Feinstein, A. Gallagher, B. IllgenWilcke, K. Pritchett-Corning, and M. Raspa. 2014. FELASA recommendations for the health monitoring of mouse, rat, hamster, guinea pig and rabbit colonies in breeding and experimental units. Lab Anim. 48: 178–192.
29. Ioan-Facsinay, A., S. J. de Kimpe, S. M. Hellwig, P. L. van Lent, F. M. Hofhuis, H. H. van Ojik, C. Sedlik, S. A. da Silveira, J. Gerber, Y. F. de Jong, et al. 2002. FcgammaRI (CD64) contributes substantially to severity of arthritis, hypersensitivity responses, and protection from bacterial infection. Immunity 16: 391–402.
30. Benonisson, H., H. S. Sow, C. Breukel, J. W. C. Claassens, C. Brouwers, M. M. Linssen, A. Redeker, M. F. Fransen, T. van Hall, F. Ossendorp, et al. 2018. FcgRI expression on macrophages is required for antibody-mediated tumor protection by cytomegalovirus-based vaccines. Oncotarget 9: 29392–29402.
31. Tutt, A. L., S. James, S. A. Laversin, T. R. Tipton, M. Ashton-Key, R. R. French, K. Hussain, A. T. Vaughan, L. Dou, A. Earley, et al. 2015. Development and characterization of monoclonal antibodies specific for mouse and human Fcg receptors. J. Immunol. 195: 5503–5516.
32. Tzeng, A., M. J. Kauke, E. F. Zhu, K. D. Moynihan, C. F. Opel, N. J. Yang, N. Mehta, R. L. Kelly, G. L. Szeto, W. W. Overwijk, et al. 2016. Temporally programmed CD8a+ DC activation enhances combination cancer immunotherapy. Cell Reports 17: 2503–2511.
33. Bruhns, P. 2012. Properties of mouse and human IgG receptors and their contribution to disease models. Blood 119: 5640–5649.
34. Hazenbos, W. L., J. E. Gessner, F. M. Hofhuis, H. Kuipers, D. Meyer, I. A. Heijnen, R. E. Schmidt, M. Sandor, P. J. Capel, M. Dae¨ron, et al. 1996. Impaired IgG-dependent anaphylaxis and Arthus reaction in Fc gamma RIII (CD16) deficient mice. Immunity 5: 181–188.
35. Drobits, B., M. Holcmann, N. Amberg, M. Swiecki, R. Grundtner, M. Hammer, M. Colonna, and M. Sibilia. 2012. Imiquimod clears tumors in mice independent of adaptive immunity by converting pDCs into tumor-killing effector cells. J. Clin. Invest. 122: 575–585.
36. Abe`s, R., E. Ge´lize´, W. H. Fridman, and J. L. Teillaud. 2010. Long-lasting antitumor protection by anti-CD20 antibody through cellular immune response. Blood 116: 926–934. 37. Dyall, R., L. V. Vasovic, R. A. Clynes, and J. Nikolic´-Zugic´. 1999. Cellular requirements for the monoclonal antibody-mediated eradication of an established solid tumor. Eur. J. Immunol. 29: 30–37.
38. Park, S., Z. Jiang, E. D. Mortenson, L. Deng, O. Radkevich-Brown, X. Yang, H. Sattar, Y. Wang, N. K. Brown, M. Greene, et al. 2010. The therapeutic effect of anti-HER2/neu antibody depends on both innate and adaptive immunity. Cancer Cell 18: 160–170.
39. Stagg, J., S. Loi, U. Divisekera, S. F. Ngiow, H. Duret, H. Yagita, M. W. Teng, and M. J. Smyth. 2011. Anti-ErbB-2 mAb therapy requires type I and II interferons and synergizes with anti-PD-1 or anti-CD137 mAb therapy. Proc. Natl. Acad. Sci. USA 108: 7142–7147.
40. Vasovic´, L. V., R. Dyall, R. A. Clynes, J. V. Ravetch, and J. Nikolic´-Zugic. 1997. Synergy between an antibody and CD8+ cells in eliminating an established tumor. Eur. J. Immunol. 27: 374–382.
41. Hara, I., Y. Takechi, and A. N. Houghton. 1995. Implicating a role for immune recognition of self in tumor rejection: passive immunization against the brown locus protein. J. Exp. Med. 182: 1609–1614.
42. Bergman, I., P. H. Basse, M. A. Barmada, J. A. Griffin, and N. K. Cheung. 2000. Comparison of in vitro antibody-targeted cytotoxicity using mouse, rat and human effectors. Cancer Immunol. Immunother. 49: 259–266.
43. Cassatella, M. A., R. M. Flynn, M. A. Amezaga, F. Bazzoni, F. Vicentini, and G. Trinchieri. 1990. Interferon gamma induces in human neutrophils and macrophages expression of the mRNA for the high affinity receptor for monomeric IgG (Fc gamma R-I or CD64). Biochem. Biophys. Res. Commun. 170: 582–588.
44. Schroder, K., P. J. Hertzog, T. Ravasi, and D. A. Hume. 2004. Interferon-gamma: an overview of signals, mechanisms and functions. J. Leukoc. Biol. 75: 163–189.
45. Narayan, R., H. Nguyen, J. J. Bentow, L. Moy, D. K. Lee, S. Greger, J. Haskell, V. Vanchinathan, P. L. Chang, S. Tsui, et al. 2012. Immunomodulation by imiquimod in patients with high-risk primary melanoma. J. Invest. Dermatol. 132: 163–169.